# Final Report for DOE-NEER Grant: DE-FG07-99ID13774

# The Adjoint Method for the Optimization of Brachytherapy and Radiotherapy Patient Treatment Planning Procedures Using Monte Carlo Calculations

D. L. Henderson
Department of Engineering Physics
University of Wisconsin – Madison
153 Engineering Research Building
1500 Engineering Drive
Madison, WI 53706

and

S. Yoo, M. Kowalok, T.R. Mackie and B.R. Thomadsen
Department of Medical Physics
and Human Oncology
University of Wisconsin-Madison
1530 Medical Sciences Center
1300 University Ave
Madison, WI 53706

October 2001

Work supported by the Office of Nuclear Energy, Science and Technology, U.S. Department of Energy under Contract No. DE-FG07-99ID13774.

## Contents

# I. Executive Summary

The goal of this project is to investigate the use of the adjoint method, commonly used in the reactor physics community, for the optimization of radiation therapy patient treatment plans. Two different types of radiation therapy are being examined, interstitial brachytherapy and radiotherapy. In brachytherapy radioactive sources are surgically implanted within the diseased organ such as the prostate to treat the cancerous tissue. With radiotherapy, the x-ray source is usually located at a distance of about 1-meter from the patient and focussed on the treatment area. For brachytherapy the optimization phase of the treatment plan consists of determining the optimal placement of the radioactive sources, which delivers the prescribed dose to the disease tissue while simultaneously sparing (reducing) the dose to sensitive tissue and organs. For external beam radiation therapy the optimization phase of the treatment plan consists of determining the optimal direction and intensity of beam, which provides complete coverage of the tumor region with the prescribed dose while simultaneously avoiding sensitive tissue areas. For both therapy methods, the optimal treatment plan is one in which the diseased tissue has been treated with the prescribed dose and dose to the sensitive tissue and organs has been kept to a minimum.

For the case of brachytherapy, a new optimization strategy was adopted based on the dose to the whole region of interest and the radioactive source influence fields. Optimization plans using this strategy showed better uniformity of dose delivery than the voxel to voxel "forward" and "adjoint" optimization methods and reduced the number of sources required for treatment. The data and storage requirements were less for the new optimization model than the voxel to voxel methods and it executed faster.

For the case of external beam radiotherapy, in this work, adjoint- and forward-based treatment plans were computed for a simplified patient model. Treatment plans for each method were calculated using a linear programming optimization scheme and compared. The objective of the comparison was to demonstrate that the "forward" and "adjoint" voxel to voxel approach would yield the same result (a benchmark for the methods). The results demonstrate that the forward and adjoint methods yield similar results within statistical error. Currently, work is focusing on optimization of using the collective response of the entire tumor region rather than on the response of individual tissue voxels. The adjoint distribution will provide an importance distribution for source position and beam direction on the circular gantry surrounding the patient.

This report summarizes the work that has taken place in these two areas over the course of the grant.

# II. Brachytherapy: Optimization for permanent prostate implantation treatment plan using forward and adjoint dose calculation methods.

## II.A Introduction

Interstitial brachytherapy is a type of radiation therapy in which radioactive sources are implanted directly into cancerous tissue. First introduced by Holm *et al.*[1], ultrasound guided permanent implantation of brachytherapy sources has become one of the leading treatment procedures for prostate cancer due to effective treatment and substantial reduction of post treatment complications as compared to other treatment methods. In this treatment approach, radioactive sources are percutaneously embedded within the prostate in a pattern that is designed to deliver a prescribed dose to the treatment region. Emphasis is placed on coverage of the diseased tissue with the prescribed dose while at the same time minimizing dose to surrounding sensitive and normal tissue. Improper placement of sources will lead either to an overdose of the surrounding tissue or an under-dose of the diseased tissue that in the long term will adversely affect the health of the patient.[2,3]

Treatment planning programs are important tools used by the radiation physicist to assist in the development of an optimal patient treatment plan. The treatment planning code uses patient specific geometry to calculate the dose to regions of interest due to placement of sources. A major challenge in brachytherapy is the difficulty of determining the optimal location for the 80 or more source implants for optimum tumor treatment.[4] Conventional treatment plans utilize single intensity strength sources and are generated by a trial and error process largely based on a clinician's expert judgment. Recently, various optimization methods such as simulated annealing, genetic algorithms and mixed integer programming based on the branch and bound algorithm have been investigated to assist the clinician with the optimization process and to automate the treatment planning process.[5 – 10] These optimization models utilize objective functions that maximize or minimize dose to the target subject to constraints that limit feasible solutions (for example, the dose to the rectum).

A critical component of the treatment planning code is the dose calculation algorithm. Conventional treatment planning uses the dose distribution formalism of AAPM TG 43[11]. This formalism uses pre-calculated values of dose distributions around a single source in a homogeneous water medium to determine the dose at a given point. Tables for this formalism come from experimental measurement of the dose distribution of the sources and/or Monte Carlo simulations. Recently, the convolution-superposition method, the discrete ordinates method, and the Monte-Carlo method have been used to compute absorbed dose from first principles in realistic patient-specific geometries. The methods compute dose including the effects of inhomogeneous media. The dose calculation using these transport methods has conventionally been performed with the "forward approach" of photon transport. In the forward approach, quantities defining source location, its strength and spectral information are known and the resulting dose distribution in the patient is calculated. An alternative dose calculation procedure is the "backward" or "adjoint approach" to photon transport. The adjoint flux computed in this manner provides a sensitivity (importance) distribution for source placement within the region of interest, which can be utilized in the optimization process

In this study, we investigate the use of the adjoint approach to optimize treatment plans to determine the optimum internal placement of an array of radioactive sources. The adjoint flux is used to compute the dose to a specific tissue Region of Interest (ROI) such as the patient's prostate and nearby urethra and rectum. But more importantly, as will be shown, it provides a sensitivity (importance) distribution for source placement within the region of interest. In addition to the adjoint fields for specific Regions of Interest (ROIs), the investigation includes the use of a "source influence field." The source influence field is the flux distribution from a single source and determines the influence of a source at one position

to other source locations. It is used in an analogous fashion as the electric field repulsive interaction between like charged particles. Sources placed in close proximity are pushed apart. This prevents sources from clustering so that a nearly uniform dose can be delivered. This approach was shown to result in a better source configuration as well as dose distribution and accelerated the optimization process. The results computed using the adjoint approach is compared to the "forward" direct source voxel to field voxel approach and the "adjoint" direct response voxel to source voxel approaches.

## II.B Background Material, Codes and Calculation Methods

### II.B.1 Ultrasound Image

A TransRectal UltraSound (TRUS) probe is inserted through the rectum for image acquisition of the prostate. An image of the organ and its surroundings is captured in transverse slices spaced 5mm apart. Fig. 1 shows one slice of prostate ultrasound image with the ROIs contoured manually by an oncologist. Four anatomical regions of interest for prostate implantation have been identified: the gray contour indicates the prostate, the white the urethra, the black the rectum and elsewhere is the normal surrounding tissue. From a treatment planning point of view the whole prostate is treated as the tumor.

The white dots in Fig. 1 correspond to points on the source implant template needle guide. The template provides a spatial reference grid for insertion of the source-loaded needles into the prostate. The dots are 0.5 cm apart in the vertical and horizontal directions indicating potential source positions. The prostate is ellipsoidal shaped with a volume of approximately 40 $cm^3$. Twelve to fifteen ultrasound image slices are obtained at 0.5 cm intervals for treatment planning.

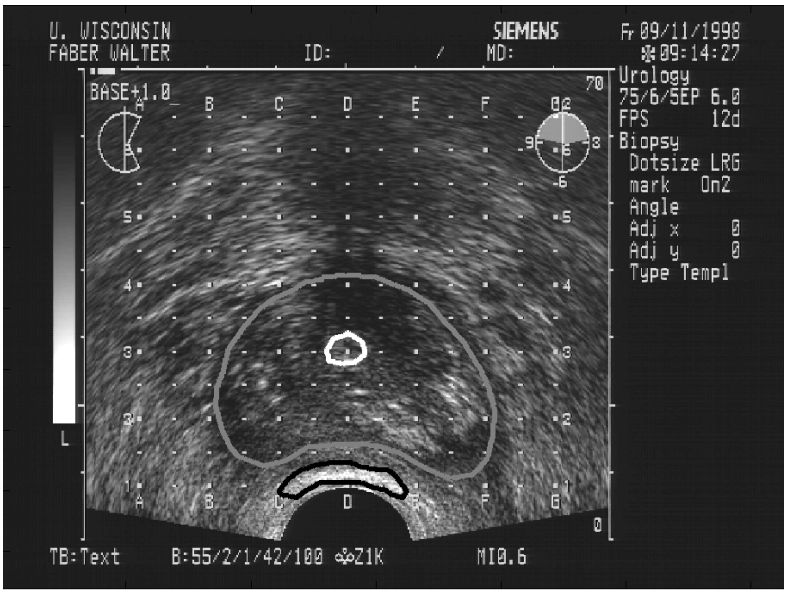


Fig 1. TransRectal Ultrasound image of the prostate with the regions-of-interest contoured. The gray contour indicates the prostate, the white the urethra, and the black the rectum

## II.B.2 Dose Calculation Methods

### Discrete ordinates code DANTSYS

A geometric model (mathematical phantom) is generated based on the contoured prostate ultrasound image shown in Fig. 1. DANTSYS, a discrete ordinates transport code, is utilized to compute the adjoint flux and the forward flux at all fine meshes (voxels) within the model.[12] For our initial investigations, a broad three group cross section library (G-3) was generated from the lowest three energy groups of the FENDL-2 42 group cross section library. The average energy of photons emitted by the most common interstitial brachytherapy radioactive seed $^{125}$I fall into the 1st group (20 - 30 keV). The 2nd and 3rd groups span the energy ranges 10 - 20 keV and 1 - 10 keV, respectively. The flux-to-dose rate conversion factors for the broad three group photon cross section library are computed using the methodology described in the American Nuclear Society standard report.[13] Typically the flux-to-dose rate conversion (CF) factor is used as the response function in a forward dose calculation. In the adjoint case, the CF is used as the adjoint source for the ROI.

### Voxel to voxel forward dose calculation method

The DANTSYS discrete ordinates code solves the Boltzmann equation [14] :

$$\hat{\Omega} \cdot \vec{\nabla} \phi(\vec{r},\hat{\Omega},E) + \mu_t(\vec{r},E) \cdot \phi(\vec{r},\hat{\Omega},E) = \int_{E'}\int_{\Omega'} \mu_s(\vec{r}, \vec{\Omega}' \rightarrow \hat{\Omega}, E' \rightarrow E) \cdot \phi(\vec{r},\hat{\Omega}',E') \cdot d\hat{\Omega}' dE' + S(\vec{r},\hat{\Omega},E) \quad (1)$$

which describes the transport of photons within and through a medium. The solution to the Boltzmann equation for the photon angular flux $\phi(\vec{r},\hat{\Omega},E)$ is known as the forward or direct solution.

The dose to a specific volumetric voxel i is the amount of energy deposited per unit mass within the region. The total dose rate to a voxel i is the double integral over all photon energies and tumor voxels of interest of the energy absorption rate divided by the mass of the voxel of interest;

$$\dot{D}_i = \int_{E'}\int_{V_i} \phi(\vec{r}',E') \cdot \mu_{en}(\vec{r}',E') \cdot E' \, d\vec{r}' \, dE' \Big/ \int_{V_i} \rho(\vec{r}') d\vec{r}' \quad (2)$$

where $V_i$ is the volume of the voxel of interest. Using the flux-to-dose rate conversion factor described in ANS-6.1.1-1977 report, the dose rate $\dot{D}_i$ to the voxel i in a discrete form is

$$\dot{D}_i = \sum_{\forall j} \sum_{g} \phi_{g,j}(i) \cdot CF_g \quad (3)$$

and the dose rate $\dot{D}_{ij}$ to the voxel i due to one source at a voxel j in a discrete form is

$$\dot{D}_{ij} = \sum_{g} \phi_{g,j}(i) \cdot CF_g \quad (4)$$

where g signifies an energy bin of multi-group energies, and $CF_g$ equals to $E \cdot \mu_{en}(E)/\rho$ for energy group g.

## Voxel to voxel adjoint dose calculation method

The adjoint equation to the Boltzmann (transport) equation in general coordinates is [14]

$$\begin{aligned} &- \hat{\Omega} \cdot \vec{\nabla} \phi^{+}(\vec{r}, \hat{\Omega}, E) + \mu_t(\vec{r}, E) \cdot \phi^{+}(\vec{r}, \hat{\Omega}, E) \\ &\quad = \int_{E'} \int_{\Omega'} \mu_s(\vec{r}, \vec{\Omega} \rightarrow \hat{\Omega}', E \rightarrow E') \cdot \phi^{+}(\vec{r}, \hat{\Omega}', E') \cdot d\hat{\Omega}' dE' + S^{+}(\vec{r}, \hat{\Omega}, E) \end{aligned} \tag{5}$$

where the function $\phi^{+}(\vec{r}, \hat{\Omega}, E)$ is known as the adjoint angular flux. $S^{+}$ is the adjoint source, which is determined from the response function of a detector in the forward solution. In the forward solution, the scalar flux is multiplied by a response function, the flux-to-dose rate conversion factor, which leads to dose rate. This response function is the adjoint source $S^{+}$ in the adjoint calculation.

The total dose rate calculation for a voxel i in the adjoint method is computed by the double integral over all energies and source area;

$$\dot{D}_i = \int_{E'} \int_{V_S} \phi^{+}(\vec{r}', E') \cdot S(\vec{r}', E') \cdot d\vec{r}' dE' \Big/ \int_{V_i} d\vec{r}' \tag{6}$$

where $V_s$ is the volume of the source and $V_i$ is the volume of the voxel i. The discrete form of the dose rate $\dot{D}_i$ due to all sources is

$$\dot{D}_i = \sum_{\forall j} \sum_{g} \phi^{+}_{g,i}(j) \cdot S_j \cdot V_j / V_i \tag{7}$$

and the dose rate $\dot{D}_{ij}$ to the voxel i due to one source at a voxel j in a discrete form is

$$\dot{D}_{ij} = \sum_{g} \phi^{+}_{g,i}(j) \cdot S_j \cdot V_j / V_i \tag{8}$$

where $V_j$ is the volume of the source voxel and $S_j$ is a source at the voxel j.

### Whole ROI Adjoint dose calculation method

The adjoint distribution for the whole ROI, $\phi^{+}_{ROI}$ is computed by placing the adjoint source $S^{+}$ in the whole ROI. Computed in this manner, the adjoint flux $\phi^{+}_{ROI}$ at a position r constitutes a dose deposition kernel for the amount of dose deposited in the ROI by a source located at the position r. The dose to a ROI is given by the following expression:

$$\dot{D}_{ROI} = \int_{E} \int_{V_s} \phi^{+}_{ROI}(\vec{r}', E') \cdot S(\vec{r}', E') \cdot d\vec{r}' \cdot dE' \Big/ \int_{V_{ROI}} d\vec{r}' \tag{9}.$$

This can be rewritten in discrete form as

$$\dot{D}_{ROI} = \sum_{\forall j} \sum_{g} \phi^{+}_{g,ROI}(j) \cdot S_j \cdot V_j \Big/ V_{ROI} \tag{10}$$

where $V_{ROI}$ is the volume of the ROI, and $V_j$ is the volume of the source voxel. This provides a means of computing the dose to the whole ROI without computing the dose to each individual pixel within the ROI. The dose rate to the ROI, $\dot{D}_{ROI,j}$, due to one source at a voxel j in a discrete form is

$$\dot{D}_{ROI,j} = \sum_g \phi^+_{g,ROI}(j) \cdot S_j \cdot V_j \Big/ V_{ROI} \tag{8}$$

Figure 2 depicts schematic views of the adjoint flux distributions for the different ROIs. The ROI adjoint flux distribution is the sensitivity of the ROI to a source at any source position j.

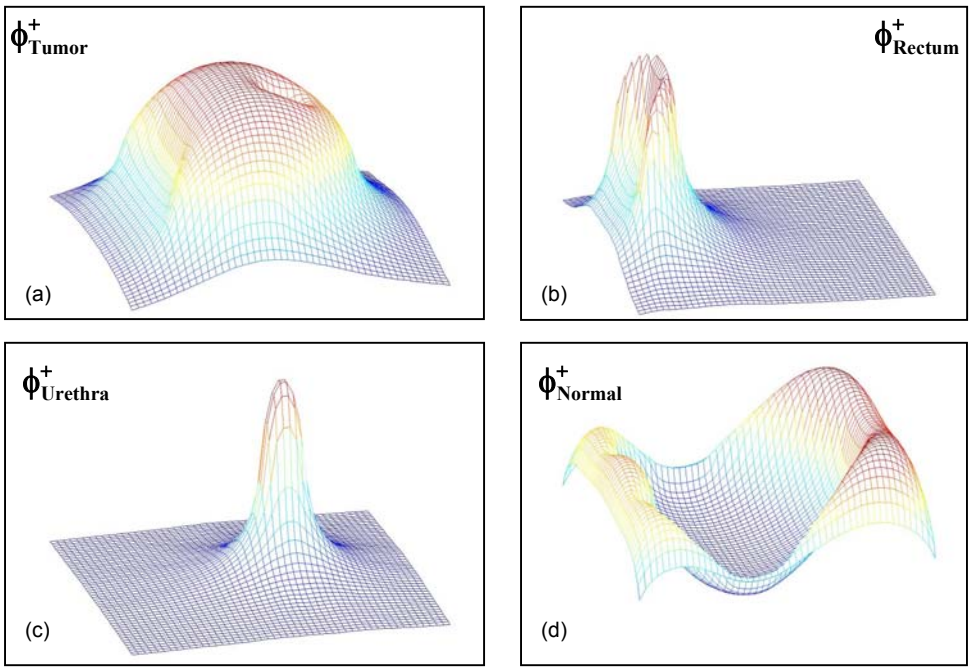


Figure 2. Whole ROI adjoint flux. (a) The whole tumor adjoint flux, (b) the whole rectum adjoint flux, (c) the whole urethra adjoint flux, and (d) the whole normal tissue adjoint flux.

## II.B.3 Optimization

### Optimization tool GAMS & Mixed integer programming

The GAMS (General Algebraic Modeling System) optimization packet is used for the optimization process in our study.[15] The pre-computed "forward approach" and "adjoint approach" dose data are utilized in GAMS to optimize treatment plans for the permanent prostate radioactive source implants. The solver employed for the optimization is the Mixed-Integer programming (MIP) branch-and-bound method. MIP can be utilized for brachytherapy problems using the binary variables 0/1 to represent source placement or non-placement that will best satisfy the prescribed dose to the tumor and dose constraints to the normal and sensitive tissues.

### Basic model

The optimizer solves an objective function by minimizing the total penalties over all dose calculation position i, [16, 17]

$$\text{minimize} \quad \sum_{\forall i} \sum_{\forall j} x_{ij} \cdot \delta_j$$

$$\text{subject to} \quad \left\{ \begin{array}{ll} \dot{D}_{ij} + x_{ij} \geq L_{tumor}, & if \quad \dot{D}_{ij} \leq L_{tumor} \quad \& \quad i \in tumor, \\ \dot{D}_{ij} - x_{ij} \leq U_{ROI}, & if \quad \dot{D}_{ij} \geq U_{ROI} \quad \& \quad i \notin tumor, \\ x_{ij} = 0, & otherwise. \end{array} \right\} \tag{9}$$

The penalty $x_{ij}$ refers to the dose difference between the calculated dose from either equation (4) or (7) and the dose constraint for the dose calculation position i due to the source at j. $L_{tumor}$ is the lower boundary of the dose to a voxel i when i is within the tumor region. $U_{ROI}$ is the upper boundary of the dose to a voxel i when i is within a ROI except the tumor. These dose constraints are determined based on the prescribed dose. If the calculated dose meets the dose constraint, then the penalty is zero so that the penalty is always greater than zero. The objective of the optimization is solving $\delta_j$ for all possible j such that the solution accomplishes the minimal total penalty. In the case no source is required, $\delta_j$ will be zero, and in the opposite case, it will be unity.

This routine requires dose calculation process using a dose function in order to check all pixels or a set of data which provide dose to the voxel i due to the source at j over all pixels implementing the objective function into the optimization routine.

### Whole ROI adjoint and source influence fields

Using equation (8), the dose to a whole ROI can be calculated and implemented into an optimization objective function. However, the dose to the whole ROI does not provide local dose information and hence, use of it without an additional constraint can cause source clustering delivering an overdose to certain areas and under-dose to other areas. To prevent this, the concept of source influence field is introduced. It is used in an analogous fashion as the electric repulsion between two like charged particles. If two sources are placed in close proximity they are pushed apart and redistribute themselves. This concept helps promote uniform dose distribution with an evenly distributed source configuration.

The optimizer solves an objective function by minimizing the total penalties over the dose to the ROI and the excess dose due to the influence fields. The mathematical expression of the objective function is

$$\text{minimize} \quad \sum_{\forall ROI} \sum_{\forall j} x_{ROI,j} \cdot \delta_j + \sum_{\forall j} \Delta\phi_j \cdot \delta_j$$

$$\text{subject to} \quad \left\{ \begin{array}{ll} \dot{D}_{ROI,j} + x_{ROI,j} \geq L_{tumor}, & if \quad \dot{D}_{ROI} \leq L_{tumor} \quad \& \quad ROI = tumor, \\ \dot{D}_{ROI,j} - x_{ROI,j} \leq U_{ROI}, & if \quad \dot{D}_{ROI} \geq U_{ROI} \quad \& \quad ROI \neq tumor, \\ x_{ROI,j} = 0, & otherwise \end{array} \right\}$$

$$\left\{ \begin{array}{ll} \sum_{\forall j'} \phi_j(j') - \Delta\phi_j \leq U_\phi, & if \quad \sum_{\forall j'} \phi_j(j') \geq U_\phi \\ \Delta\phi_j = 0, & otherwise. \end{array} \right\} \tag{10}$$

where the term $\Delta\phi_j$ is an expression for the excessive amount of the source influence to a source position j due to sources at all sources j' including j. The use of the whole ROI dose term $\sum_{\forall ROI}\sum_{\forall j} x_{ROI,j}\cdot\delta_j$ reduces the data requirements from the basic model $\sum_{\forall i}\sum_{\forall j} x_{ij}\cdot\delta_j$. The former computes the dose to each ROI to meet the dose constraints whereas the later calculates the dose to each pixel to fulfill the constraints. The additional source influence term $\sum_{\forall j}\Delta\phi_j\cdot\delta_j$ does not require computation for each pixel but scans only possible source positions that are limited by the template grid which appear every 0.5 cm x 0.5 cm within the tumor region. The upper boundary constraint, $U_\phi$, is set for the source influence field based on the maximum value of $\phi_j(j')$. The dose to each pixel should be computed using equation (4) after the optimization solves the source configuration.

## II.C Results

The forward flux and adjoint flux were computed in a 50 x 50 matrix tissue material phantom with 0.1 cm x 0.1 cm pixel resolution. There are four ROIs: tumor, urethra, rectum and normal tissue. 150Gy was prescribed to the tumor treated with 0.3 mCi sources.

Two different combinations of the dose constraints were simulated.

### Case I

The dose constraints for the objective function were 150% of 150Gy (225Gy) for the lower tumor dose boundary ($L_{tumor}$), 150% of 150Gy (225Gy) for the upper urethra dose boundary ($U_{urethra}$), 125% of 150Gy (187.5Gy) for the upper normal tissue dose boundary ($U_{normal}$), and 80% of 150Gy (120Gy) for the upper rectum dose boundary ($U_{urethra}$). These limits are based on radio-biological characteristics of an organ and the prescribed dose.

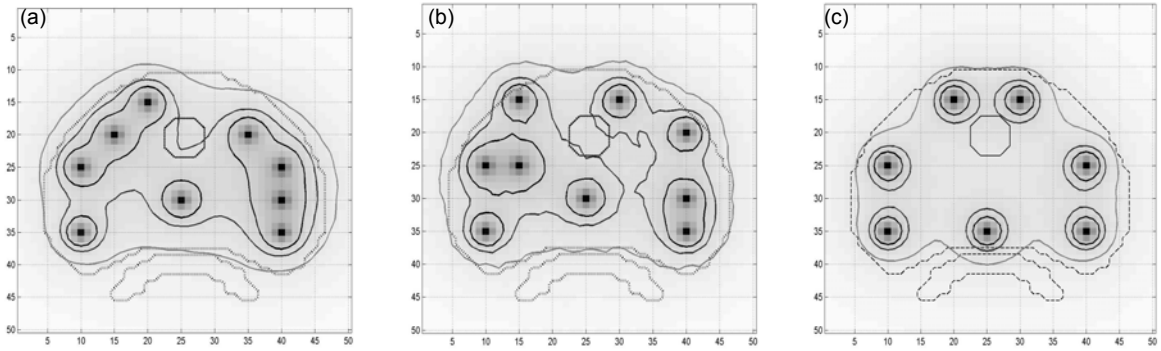


Figure 3. Isodose curves comparing the two optimization objective functions. (a) is the result of the basic optimization model using voxel-to-voxel forward dose calculation method and (b) is the result of the basic optimization model using voxel-to-voxel adjoint dose calculation method. (c) is the result of the optimization model using the whole ROI adjoint fields and the source influence field. The dotted lines are the tumor, the rectum and the urethra. The solid lines from interior region to outer region are 200%, 150%, and 100% isodose of the prescribed dose 150Gy. The black dots are the sources.

Figure 3 shows isodose curves for the two objective functions, a basic objective function used for optimizing both the forward (a) and adjoint (b) voxel to voxel dose calculation data and (c) the optimization result of the objective function using the dose to whole ROIs and the source influence fields. In Fig. 3c the sources are more evenly distributed over the tumor region compared to figures 3a and 3b, which depict source clustering within the tumor. A total of 9 sources were used for the treatment plans computed for the basic optimization models (Figs. 3a and 3b). The optimization model with the whole ROI adjoint and the source influence fields used 7 sources. However, in (c), there are some regions in the tumor receiving less than the prescribed dose, which will result in an incomplete treatment. In case II we increase the dose constraints, which as will be shown, will lead to an improved treatment plan.

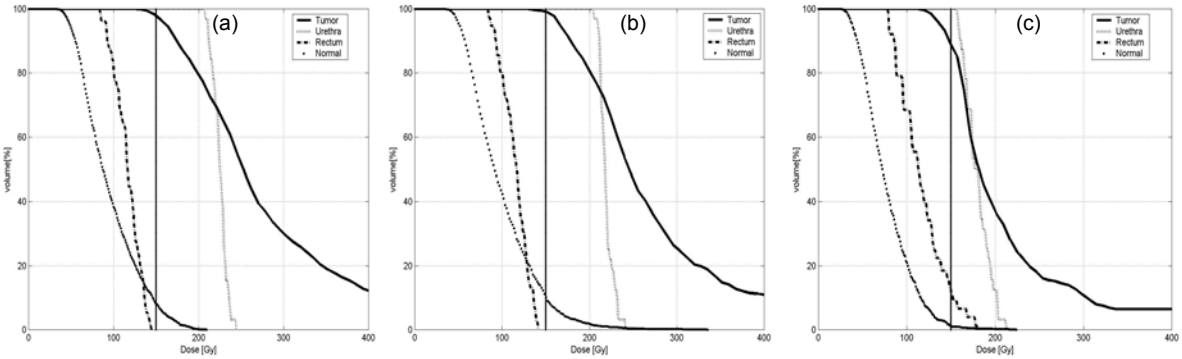


Figure 4. DVHs comparing the two optimization objective functions. (a) and (b) are the result of the basic objective function using the dose calculation to each pixel. (c) is the result of the objective function using the dose to a whole ROI and the source influence field. The ordinate is the volume of ROIs in % and the abscissa is the dose in Gy. The solid vertical line is the prescribed dose line at 150Gy.

A measure of the quality and effectiveness of the treatment plan is given by the Dose Volume Histogram (DVH). Shown in figure 4 are the DVH curves for the three methods investigated: (a) the basic optimization model with the forward dose calculation method, (b) the basic optimization model with the adjoint dose calculation method, and (c) the optimization model using the dose to whole ROIs and the source influence field. The slope of the solid DVH (tumor DVH) in figure 4c drops off quickly as the dose increases after reaching the prescribed dose which means more uniform dose whereas the tumor DVH curves in figure 4a and 4b have slowly diminishing slopes. The optimized treatment plan based on the whole ROI adjoint field and the source influence field does not achieve the prescribed dose delivery to 100% of the tumor volume. As depicted in figure 4c, about 90% of the tumor receives the prescribed dose. The tumor DVH in figure 4a also indicates the prescribed dose was not delivered to the complete tumor volume. Hence we increase the dose constraints in the objective functions to improve the treatment plan.

## Case II

The dose constraints in case I were not successful in delivering the prescribed dose to the tumor as shown in figure 3 and 4 (a) and (c). Thus the dose constraint for the tumor dose was raised to 180% of 150Gy (270Gy) for the lower tumor dose boundary ($L_{tumor}$) while retaining the other constraints the same as for cases I.

Figure 5 depicts the isodose curves for the two objective functions, a basic objective function used for optimizing both the forward (a) and adjoint (b) voxel to voxel dose calculation data and (c) the optimization result of the objective function using the dose to whole ROIs and the source influence fields.

As in the previous case, sources are more evenly distributed throughout the tumor region in figure 5c whereas figures. 5a and 5b show source clustering in certain regions. A total of 10 sources were used for the treatment plans by the basic optimization model (figure 5a and 5b). In comparison the optimization model with the whole ROI adjoint and the source influence fields used 9 sources (figure 5c). The increase in the dose constraint for the tumor allowed for the complete prescribed dose delivery to the entire tumor region without a cold spot. However, shown in the figure 4a and 4b, these treatment plans require more sources than depicted in figure 4c. A reduction in the number of sources was also noted for case I (figure 3c).

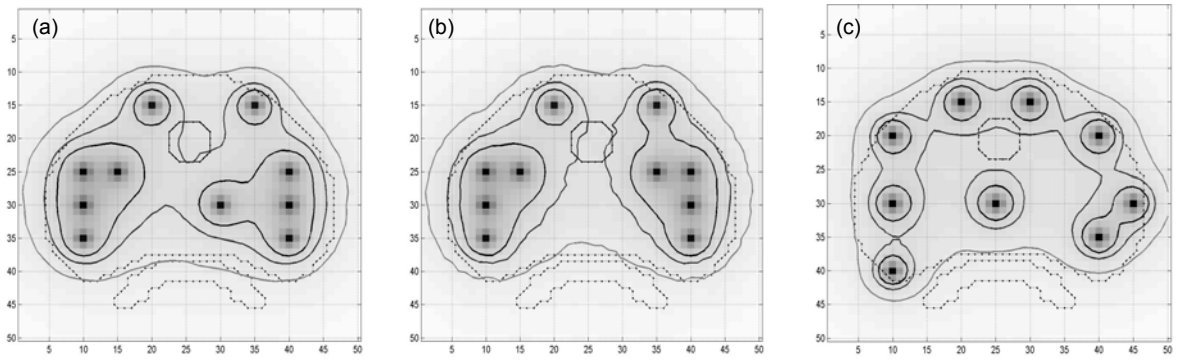


Figure 5. Isodose curves comparing the two optimization objective functions. (a) is the result of the basic optimization model using voxel-to-voxel forward dose calculation method and (b) is the result of the basic optimization model using voxel-to-voxel adjoint dose calculation method. (c) is the result of the optimization model using the whole ROI adjoint fields and the source influence field. The dotted lines are the tumor, the rectum and the urethra. The solid lines from interior region to outer region are 200%, 150%, and 100% isodose of the prescribed dose 150Gy. The black dots are the sources.

In figure 5c, the source configuration is more evenly spread over the entire tumor region compared to (a) and (b). The source influence field in the objective function (10) plays an important role in preventing the sources from clustering as well as reducing the number of sources required for the treatment. The slope of the solid DVH (tumor DVH) in figure 6-(c) drops off quickly as the dose increases after reaching the prescribed dose whereas the tumor DVHs in figure 6a and 6b have slowly diminishing slopes. The prescribed dose 150Gy was delivered to 100% of the tumor volume in all treatment plans shown in figure 6.

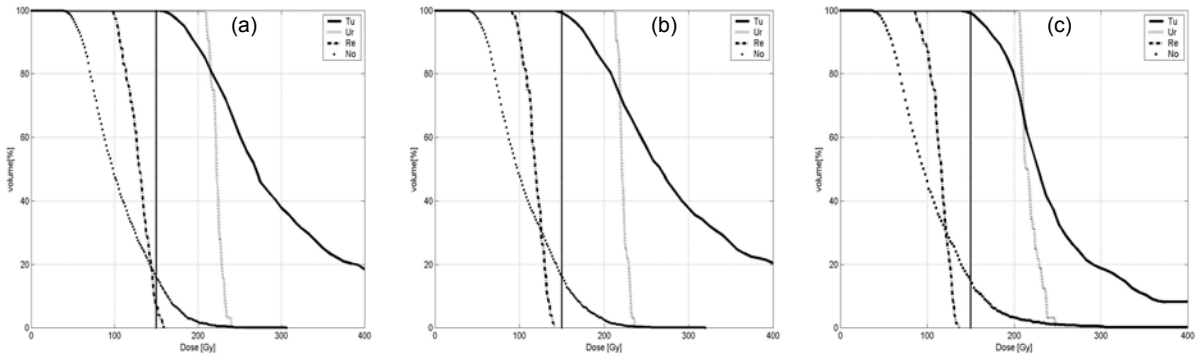


Figure 6. DVHs comparing the two optimization objective functions. (a) and (b) are the result of the basic objective function using the dose calculation to each pixel. (c) is the result of the objective function using the dose to a whole ROI and the source influence field. The ordinate is the volume of ROIs in % and the abscissa is the dose in Gy. The solid vertical line is the prescribed dose line at 150Gy.

## II.D Discussion

In this study we investigated the use of the adjoint approach to optimize treatment plans to determine the optimum internal placement of an array of radioactive sources. The results computed using the adjoint approach coupled with the "source influence field" repulsive interaction were compared to the "forward" direct source voxel to field voxel and the "adjoint" direct response voxel to source voxel approach. For the adjoint approach coupled with the repulsive source field, it was found that the sources were more evenly distributed over the tumor region compared to the latter methods and a more uniform dose field was produced. It was also noted that the number of sources required for the optimization was reduced over that used in the direct methods. Because the dose to only the whole ROIs is included in the optimization process, our optimization model requires one more procedure to compute the local dose distribution compared to the other two methods. The dose to each pixel is computed after the optimal source configuration has been determined. However, once the source positions have been determined, it doesn't take long to compute dose. The new optimization model investigated required 40 Kb of data executing $8.8*10^4$ iterations to reach the optimal solution while the basic model required 2.2 Mb of data executing $2.2*10^6$ iterations to achieve the optimal solution. The basic model takes about 10 to 20 times longer processing time on a Compaq XP1000 alpha 667MHz machine having 512Mb of memory.

## II.E Future work

The broad 3 group cross-section library (G-3) was used to simulate the implantation sources $^{125}$I and $^{103}$Pd. The 210 group cross section library (G-210) provided by NRC-CNRC will be implemented into the discrete ordinate system for accurate source simulation and dose computation.[18]

This study has been performed in two-dimensional geometry as a first step. In order to apply for clinical uses the treatment plan optimization should be executed with 3-dimensional geometry and compared with the conventional commercial treatment planning system. We are currently in the process of expanding to 3-dimensional calculations.

## II.F References:


1. H. H. Holm, N. Juul J. F. Pedersen, H. Hansen, *et. al*., "Transperineal I-125 iodine seed implantation in prostatic cancer guided by transrectal ultrasoundgraphy", J. Urol. (Baltimore) 130, 283 – 296 (1983).
2. Glenn P. Glasgow, "Isodose Planning: brachytherapy," Treating Planning in *Radiation Oncology*, Chap. 11, Williams and Wilkins, Copyright 1998.
3. G. A. Ezzell and R. W. Luthmann, "Clinical Implementation of Dwell Time Optimization for Single Stepping-Source Remote Applications," Brachytherapy Physics, Chap.~30, Medical Physics Publishing Corporation, Madison, Wisconsin, Copyright 1994.
4. E. K. Lee, *et al*., "Treatment planning for brachytherapy: an integer programming model, two computational approaches and experiments with permanent prostate implant planning," *Phys. Med. Biol.*, 44, 145 – 165 (1999)
5. Y. Yu, M. C. Schell, "A genetic algorithm for the optimization of prostate implants", Med. Phys. 23 (12), Dec 1996: 1085 – 2091.
6. G. Yang, L.E. Reinstein, S. Pai, *et al*., "A new genetic algorithm technique in optimization of permanent $^{125}$I prostate implants", Med. Phys. 25 (12), Dec, 1998: 2308- 2315.
7. M. Zaider, M. J. Zelefsky, E. K. Lee, *et al.*, "Treatment planning for prostate implants using magnetic-resonance spectroscopy imaging", Int. J. Radiation Oncology Bio. Phys., Vol 47, No. 4. 1085 – 1096, 2000.

8. E. K. Lee, R. J. Gallagher, D. Silvern, *et al.*, "Treatment planning for brachytherapy: an integer programming model, two computational approaches and experiments with permanent prostate implant planning", Phys. Med. Biol, 44 (1999) 145- 165.
9. W. D. D'Souza, R. R. Meyer, B. R. Thomadsen, *et al.*, "An iterative sequential mixed-integer approach to automated prostate brachytherapy treatment plan optimization", Phys. Med. Biol, 46(2001) 297-322
10. E. K. Lee, T. Fox, and I. Crocker, "Optimization of radiosurgery treatment planning via mixed integer programming", Med. Phys., 27(5) May 2000: 995-1004
11. R. Nath, L.L. Anderson, G. Luxton, K.A. Weaver, J.F. Williamson, A.S. Meigooni, ``Dosimetry of interstitial brachytherapy sources: Recommendations of the AAPM Radiation Therapy Committee Task Group No. 43", Med. Phys. vol. 22, 209-234 (1995).
12. DANTSYS: A Diffusion Accelerated Neutral Particle Transport Code System," Los Alamos National Laboratroy Report, LA-12969-M (June 1995).
13. "Neutrons and gamma-ray flux-to-dose-rate factors", ANSI/ANS-6.1.1-1977.
14. G. Bell, S. Glasstone, Nuclear Reactor Theory, Chap. 6, Robert E. Krieger Publishing Company, Huntington, New York (1979).
15. "GAMS Language guide", GAMS Development Corporation, 1997.
16. Nemhauser, Wolsey, Integer and Combinatorial Optimization, published by John Wiley. ISBN TBD.
17. Parker, Rardin, Discrete Optimization, published by Academic Press. ISBN TBD.
18. G. M. DasKalov, R. S. Baker, R. C. Little, *et. al.,* "Two-Dimensional Discrete Ordinate Photon Transport Calculations for Brachytherapy Dosimetry Applications", Nucl. Sci. Eng., 1999.

# III. Radiotherapy: Therapy Treatment Planning using Monte Carlo Transport

## III.A Introduction

The general goal of external beam radiation therapy is to deliver a prescribed dose to tumor tissue, while minimizing the dose to adjacent healthy tissues. Radiation therapy treatment planning is the process of determining the beam directions and beam intensities that will deliver the distribution of dose as prescribed. This process requires the optimization of a radiation source in terms of position, direction, and intensity.[1-4]

Forward and adjoint transport methods can each be used to generate the data necessary for treatment planning. In general, forward methods transport a source function to all possible detector locations, while adjoint methods transport the response function of a detector to all possible source positions. For external beam therapy, the detectors are the patient's tissues, and the response function is the tissue flux-to-dose conversion factor. The source is a megavoltage x-ray beam that can be aimed at the patient from different directions. For a single source direction, forward-based transport can determine the dose at every point in the patient. One forward calculation must be performed for each source direction. Alternatively, for a single point in the patient, adjoint-based transport can determine the dose at that point from every possible source direction simultaneously.[5, 6] One adjoint calculation must be performed for each point of interest in the patient. Given that the desired dose for all points of interest is known *a priori* for every radiation therapy problem, adjoint methods lend themselves in a natural way to the treatment planning process.[7]

In this work, adjoint- and forward-based treatment plans were computed for a simplified patient model. Treatment plans for each method were calculated using a linear programming optimization scheme. The adjoint- and forward-based methods are discussed in terms of methodology and end results.

## III.B Methods and Materials

### Adjoint Transport Equation and Dose Calculations

The importance of particles throughout a system in contributing to a detector's response is given by the adjoint function for that detector, and is described by the adjoint form of the Boltzmann transport equation.[8-10] For the steady state case with a non-multiplying medium, this expression is:

$$-\vec{\nabla}\cdot\hat{\Omega}\psi^{+}(\vec{r},\hat{\Omega},E)+\Sigma_t(\vec{r},E)\psi^{+}(\vec{r},\hat{\Omega},E) = \int\int\Sigma_s(\vec{r},\hat{\Omega}\to\hat{\Omega}',E\to E')\psi^{+}(\vec{r},\hat{\Omega}',E')d\Omega' dE' + S^{*}(\vec{r},E,\hat{\Omega}).$$

The unknown dependent variable $\psi^{+}(\vec{r},\hat{\Omega},E)$ is the angular flux of adjoint particles, and describes the spatial, angular, and energy dependence of the detector response function within the medium. For the radiotherapy problem, this response function is the scalar flux-to-dose-rate conversion function *(rem / hr)/(γ /cm$^2$·sec)*. With these units, the units for adjoint flux are *(rem / hr)/(γ $^+$/cm$^3$·sec)*, where γ $^+$ denotes an adjoint particle. In adjoint transport, adjoint particles are viewed as scattering backwards and gaining energy while traveling backwards from the detector to the source.[11]

Solutions to the adjoint transport equation can be used to calculate the source that will give a desired detector response. The dose $D$ delivered to a given voxel by a source distribution S may be expressed as an inner product of the source distribution and the adjoint function $\psi^+$:

$$D = < S \, \psi^+ > \qquad (1)$$

Values of the response function were extracted from American National Standard *Neutron and Gamma-Ray Flux-to-Dose-Rate Factors.*[12]

### Forward Transport Equation and Dose Calculations

The influence of a source within a medium is given by the forward form of the Boltzmann transport equation:

$$\vec{\nabla} \cdot \hat{\Omega} \psi(\vec{r}, \hat{\Omega}, E) \; + \; \Sigma_t(\vec{r}, E) \psi(\vec{r}, \hat{\Omega}, E)$$

$$= \int\int \Sigma_s(\vec{r}, \hat{\Omega} \rightarrow \hat{\Omega}', E \rightarrow E') \; \psi(\vec{r}, \hat{\Omega}', E') \, d\Omega' \, dE' \; + \; S(\vec{r}, E, \hat{\Omega})$$

where $\psi(\vec{r}, \hat{\Omega}, E)$ is the particle flux differential in energy $E$ and direction $\Omega$ at location **r**.

The dose $D$, delivered by a source $S$ may be expressed as an inner product:

$$D = < \psi \, S^+ > \qquad (2)$$

where the notation $S^+$ refers to the response function of the medium. From this notation, the forward and adjoint method are related to each other through dose[13] as follows:

$$D = < \psi \; S^+ > = < S \, \psi^+ >$$

### Treatment Planning with Adjoint and Forward Methods

The treatment planning process begins with a CT scan of the patient. This scan discretizes the patient's anatomy into a matrix of voxels and reports the electronic density of the tissue in each voxel. For this discussion, let $i$ be an index that runs through all of the voxels, and $j$ be an index that runs over all possible source positions.

The adjoint approach will transport the response function of a single voxel $i$ to all source positions $j$. The magnitude of the adjoint flux at a particular source position $j$ represents the dose in $i$ per unit source at $j$. This sensitivity, denoted as $\psi^+_{i,j}$, can be determined at all phase space positions $j$ in a single transport computation. One transport computation must be done for each patient voxel that is of interest. From these computations a linear system that relates the dose and source distributions can be written as:

$$\overline{D_{voxel_i}} = \overline{\overline{\psi^+_{i,j}}} \; \overline{S_{position_j}} \qquad (3)$$

where the transfer matrix $\psi^+_{i,j}$ has values of dose per unit source, and $S$ is the weighting distribution for the source at all positions $j$.

The forward approach constructs the transfer matrix by transporting particle flux from each source position to every patient voxel. One transport computation must be done for each possible source position and direction. The linear system resulting from the forward method is written as:

$$\overline{D_{voxel\ i}} = \overline{\overline{d_{i,j}}}\ \overline{S_{position\ j}} \qquad (4)$$

where the transfer matrix $d_{i,j}$ has values of dose per unit source, and $S$ is the weighting distribution for the source at all positions $j$.[14] As shown in equation 2, each value in the $d_{i,j}$ transfer matrix is found by the product of $\psi$, the forward flux within the voxel, and $S^+$, the flux-to-dose conversion factor.

Since the desired dose distribution is known in each case, the treatment-planning problem may be solved mathematically by inverting the transfer matrix in equation 3 or 4, and then solving for the distribution of beam weights $S$. In practice however, the fact that all radiation sources must have non-negative intensities generally precludes this inversion from returning a feasible solution. Hence, treatment planning is essentially an optimization problem.

## Source Optimization

Optimized solutions for the linear systems of equations 3 or 4 may be found with the aid of a mathematical programming model.[15] In this work, a linear programming model and the General Algebraic Modeling System (GAMS)[16] was used to implement and solve the treatment planning problem. GAMS is a high-level modeling system consisting of a language compiler and a family of integrated high-performance solvers.

The linear programming model was of the form:

$$\text{minimize:} \quad \sum_{i,j} \left( p^{TU}_{\ i,j} + \theta_{SS} \cdot p^{SS}_{\ i,j} + \theta_{NT} \cdot p^{NT}_{\ i,j} \right) \qquad (5)$$

$$\text{subject to:} \quad \psi^{+}_{\ i,j} \cdot S_j + p^{TU}_{\ i,j} \geq d_i^{\ prescribed\ TU} \quad \forall\ voxels_i \in TU \qquad (5a)$$

$$\psi^{+}_{\ i,j} \cdot S_j - p^{SS}_{\ i,j} \leq d_i^{\ prescribed\ SS} \quad \forall\ voxels_i \in SS \qquad (5b)$$

$$\psi^{+}_{\ i,j} \cdot S_j - p^{NT}_{\ i,j} \leq d_i^{\ prescribed\ NT} \quad \forall\ voxels_i \in NT \qquad (5c)$$

where the objective function to be minimized (eq. 5) is a sum of penalty functions $p^{TU}$, $p^{SS}$, and $p^{NT}$. The superscripts in the constraint equations (5a-5c) refer to the different tissue types evident within the patient CT scan; tumor (TU), sensitive structure (SS), and normal tissue (NT). In general, the therapeutic dose prescription specifies different dose constraints for each tissue type. Since tumor tissue must not be under dosed, equation 5a registers a penalty for each tumor voxel in which the dose delivered is less than the dose prescribed for tumor voxels. Similarly, equations 5b and 5c register penalites for voxels in which the dose delivered is greater than the prescribed dose constraint for sensitive structure voxels (such as the spinal cord) and for normal tissue voxels. The optimizer thereby seeks a source configuration that results in the minimum sum of these penalties.

The factors $\theta_{SS}$ and $\theta_{NT}$ are normalization weights computed by dividing the number of SS-type (or NT-type) tissue voxels by the number of TU-type voxels. This weighting scales the optimization so that no one tissue type dominates the solution at the expense of another tissue type. These weights may be further adjusted in a trial-and-error process to further improve optimizer performance. Finally, a non-negativity constraint is required for all source weights $S_j$.

## Monte Carlo Model for Adjoint and Forward Transport

The Monte Carlo code MCNP[17] was used for forward and adjoint transport simulations with a simplified patient geometry. As shown in Figure 1, a homogenous block phantom (31x31x11 cm) of unit-density water was located at the center of a cylindrical surface 1 cm wide and 100 cm in radius. Figure 2 shows

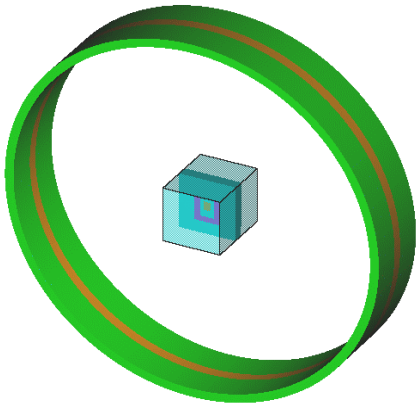

**Figure 1**

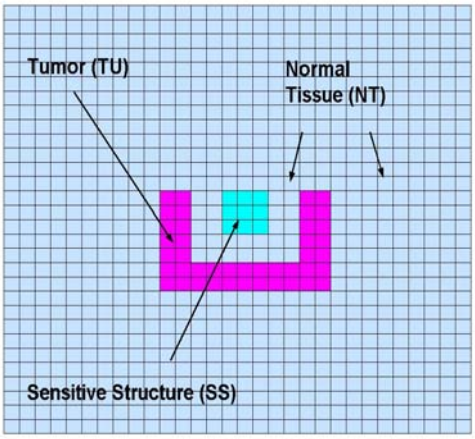


**Figure 2**

that the central slice of this phantom was divided into a lattice of $1cm^3$ voxels and that tumor-type voxels are arranged in a C-shape around a sensitive structure. The goal for the treatment plan was to deliver a dose of 60 Gy to the tumor while sparing the sensitive structure and normal tissue as much as possible.

When the model was run in adjoint mode, an adjoint flux surface-crossing tally was specified along 36 segments of the cylindrical surface shown in Figure 1. The segments were equally spaced around the surface and each segment subtended an arc length of 0.61 cm. Figure 3 shows an example of this surface-crossing tally for one simulation at 9 of the 36 scoring segments. This tally was binned into

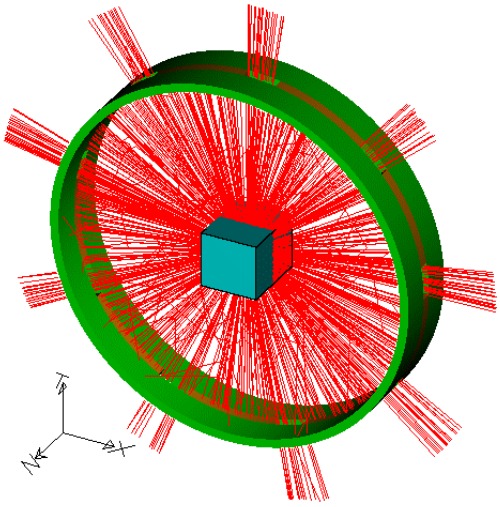

**Figure 3**

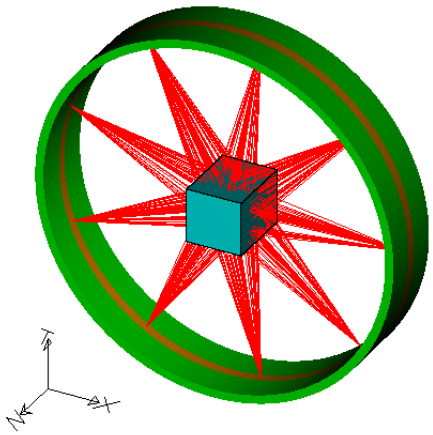

**Figure 4**

different crossing directions with each direction binned again by energy.

When the model was run in forward mode, the cylindrical surface shown in Figure 1 specified the position of 36 possible surface sources, with 21 directions available at each position. The arc length and position of the 36 surface sources corresponded exactly with the arc length and positions of the segments used for the adjoint flux surface crossing tallies. Figure 4 shows 9 of the 36 possible source positions, with each source shining into all 21 possible directions simultaneously.

The energy bin structure for adjoint and forward simulations matched the default energy group structure for MCNP multigroup adjoint transport.[18] The energy spectrum for the adjoint source was determined by integrating the energy-dependent flux-to-dose-rate factor over each multigroup energy bin. The energy response of the surface crossing tally was matched to the energy spectrum for a 6 MV therapeutic x-ray source available from a hospital-based linear accelerator.[19] Hence, when run in adjoint mode, the adjoint source had the energy spectrum of the response function from the forward problem, and the energy response for the adjoint tally had the energy spectrum of the source from the forward problem. Alternatively, when the model was run in forward mode, the forward source had the energy spectrum of a therapy beam, and the energy response for the flux tally in each patient voxel was the ANS flux-to-dose conversion factor.

## III.C Results and Discussion

### Dose per Unit Source

Tally results for forward and adjoint simulations are shown in Figures 5a through 5c. Results from forward simulations are shown on the left, while adjoint tallies are shown on the right. For each forward simulation, the source was positioned at 12:00 o'clock and the dose per unit source for every voxel is shown simultaneously. From a beam's-eye-view, the direction of the source ranges from the far right in Figure 5a to the far left in Figure 5c. For each adjoint simulation, the surface crossing tally was positioned at 12:00 o'clock and the dose in each patient voxel per unit source at this tally location and direction is shown simultaneously. From the patient's-eye-view, the direction bin for the tally ranges from the far right in Figure 5a to the far left in Figure 5c.

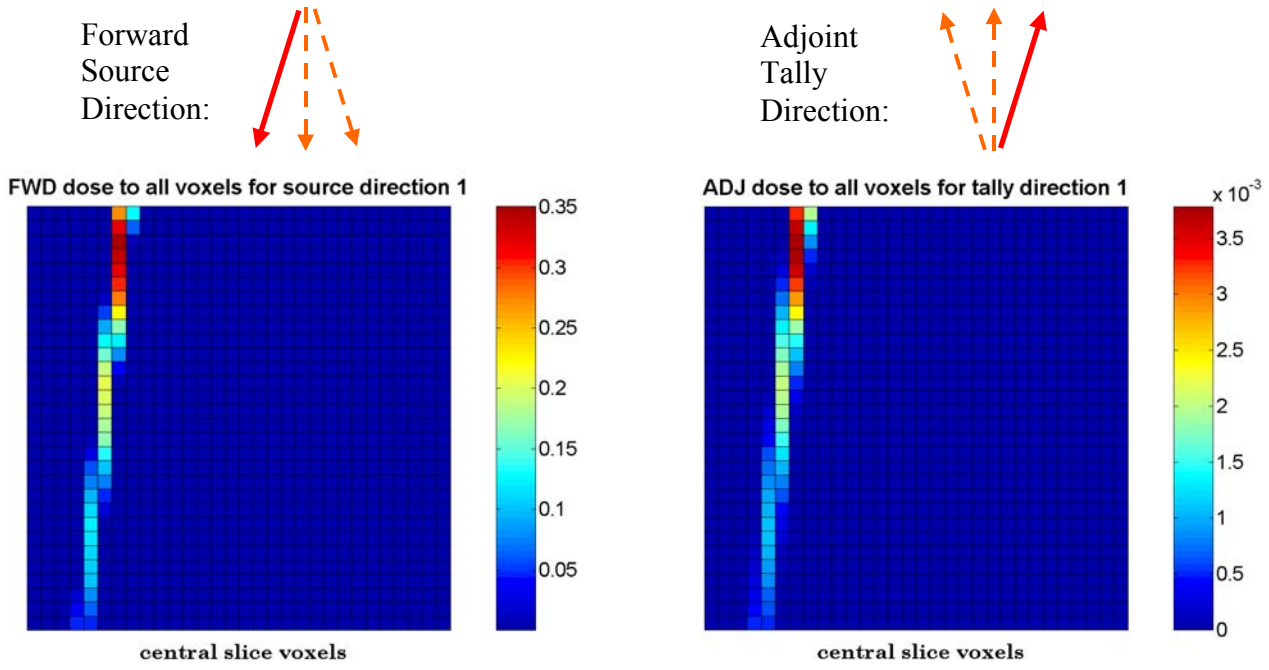


Figure 5a

Results from the forward runs on the left indicate that the dose in a patient voxel is elevated only if the voxel is along a line-of-sight with the source direction. Results from the adjoint runs indicate that for each patient voxel, the magnitude of the surface crossing tally for the direction bin indicated is elevated

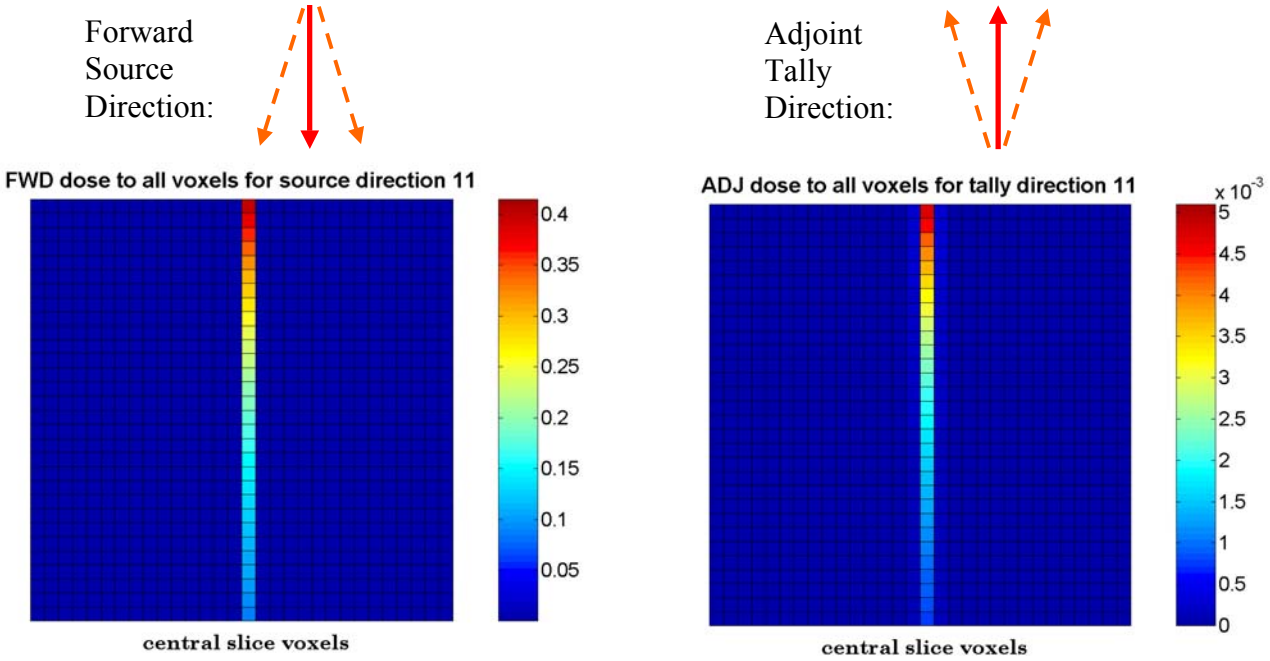


Figure 5b

only if the bin's direction is along a line-of-sight with the patient voxel. Hence, the dose in a patient voxel is elevated only if the voxel is along a line-of-sight with the tally direction; voxels not on such a line-of-sight have little sensitivity to a source located at the tally's position in phase space.

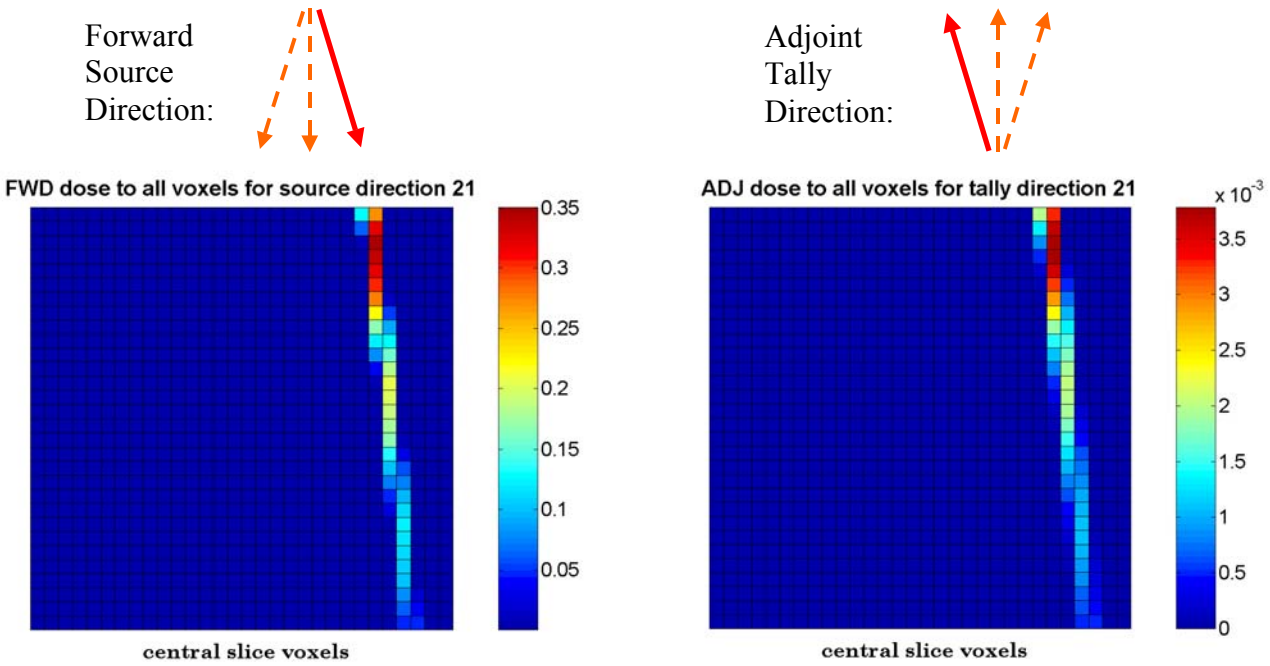


Figure 5c

Although the interpretations for the forward and adjoint tallies are slightly different, the data for both cases behave exactly the same. This similarity should be expected given that both problems were run with the same energy groups and cross-section data. The results differ in absolute magnitude because a normalization factor has not been applied to the adjoint data. This normalization factor is a constant that accounts for differences in the source density and response function for forward and adjoint modes.[18] Otherwise, the absolute magnitudes of the forward and adjoint results should differ only within the range of statistical noise on the tallies. For adjoint tallies, the magnitude of this noise varies from 0.007 to 0.015 for 50,000,000 starting particles. For forward tallies, the noise varies from 0.000012 to 0.0035 for 500,000 starting particles. The adjoint tallies have larger errors because adjoint particles must be transported into $4\pi$ while the adjoint surface crossing tally is defined only over a small surface area.

**Optimized Source Weights and Resultant Dose Distributions**

The source distributions calculated by the optimizer are shown in Figure 6. The treatment plan for the forward case is shown on the left, while the plan for the adjoint case is shown on the right. Each plan is a map of the weights assigned to every possible source position and direction. The 36 possible source positions are listed along the ordinate, while the 21 directions for each possible position are shown along the abscissa.

The two intensity maps are similar to each other and are consistent with our geometric model. That is, from Figure 2 and Figure 5b, we can see that direction number 11 is directed normally into the patient and is therefore aimed directly at the sensitive structure. From Figure 6, we can see that direction number 11 is unused for all source positions. Hence, the optimizer has calculated a plan so that no source shines exactly at the sensitive structure. Similarly, from Figures 2, 5a, and 5c, we can see that source directions 1 through 4 and 18 through 21 do not shine on the tumor. Hence, the optimized plan has a zero weighting for these directions at all source positions.

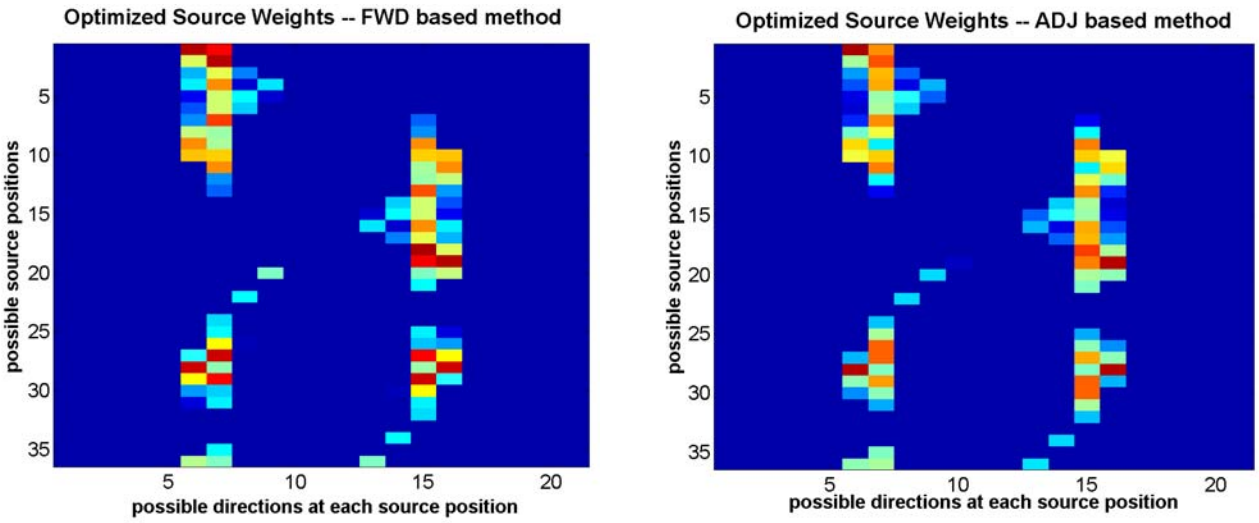


Figure 6

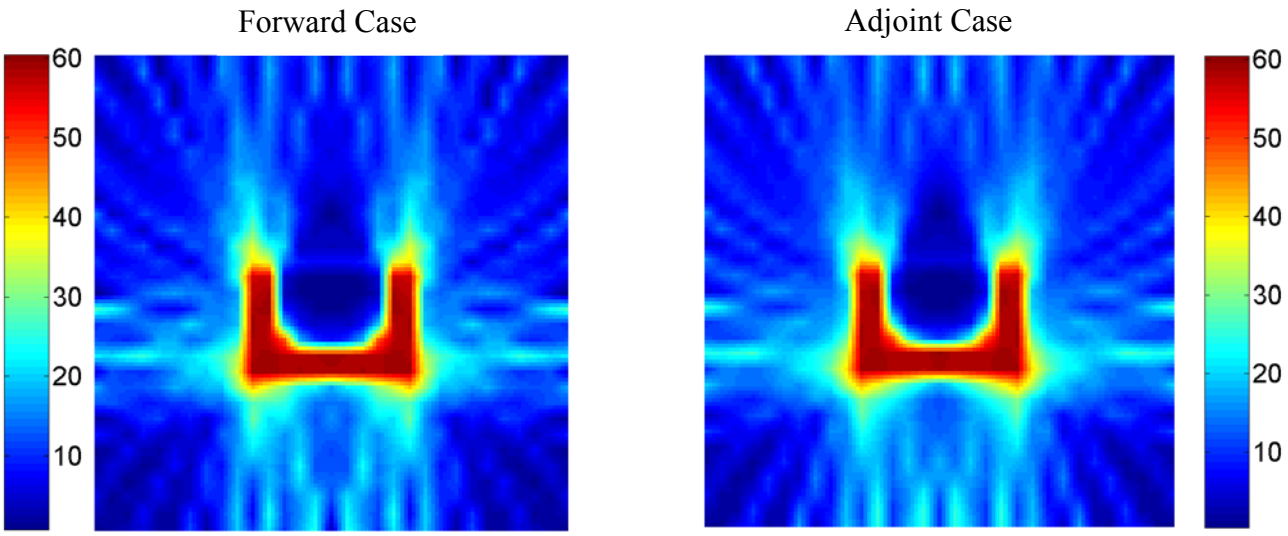


Figure 7

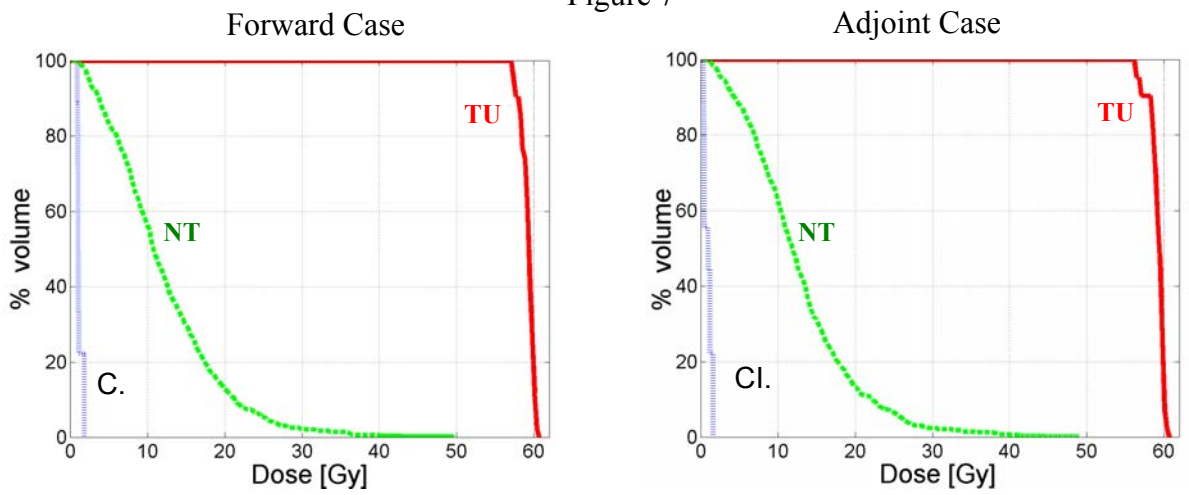


Prescription: **TU = 60 Gy; SS = 0 ; NT = 0**

Figure 8

The dose distributions resulting from the calculated source distributions are shown in Figure 7. These dose distributions indicate that most of the tumor region appears to be elevated to the prescribed dose of 60 Gy, while little dose has been delivered to the sensitive structure.

The dose volume histograms (DVHs) shown in Figure 8 provide a more quantitative review of these treatment plans. The DVH reports the fraction of each tissue type that is raised to each dose level, and is one way to evaluate a treatment plan. In general, superior plans have tumor DVHs that are completely flat at 100% but then drop to zero as a step function exactly at the prescribed tumor dose. Superior plans also have sensitive structure and normal tissue DVHs that show only small volumes raised to larger doses.

The DVH for the forward case and for the adjoint case indicate that large fractions of the tumor are raised to high doses while most of the sensitive structure is spared from high doses. These results could be improved by making adjustments in the optimization scheme such as changing the values of $\theta_{SS}$ and $\theta_{NT}$ in the objective function (eq. 5) of the linear programming model.

## III.D Conclusions

External beam radiation therapy treatment planning is the process of determining the beam directions and beam intensities that will deliver a prescribed dose distribution. In this work, adjoint-based and forward-based treatment plans were computed for a simplified patient model. Treatment plans for each method were calculated using a linear programming optimization scheme. This effort demonstrated that adjoint methods can be used as the basis for radiation therapy treatment planning, and that the optimized results from the adjoint approach are quite similar to those from the forward approach within statistical error.

The adjoint method required one transport calculation for each patient voxel of interest. Each adjoint calculation transported a response function into $4\pi$, and required a surface-crossing tally at every possible source position. The forward-based method required one transport calculation for every possible source position. Each forward calculation transported a source into a narrow solid angle and required a flux tally in every patient voxel of interest.

The statistical noise for adjoint tallies is larger than the noise on forward-based tallies. This difference is due to the $4\pi$ geometry for adjoint transport and to the fact that adjoint tallies are defined over only small surface areas. Hence, for the same tally statistics, adjoint simulations are more computationally expensive than forward runs.

## III.E Future Work

Future work will focus on optimization using the collective response of an entire tumor region rather than on the response of individual tissue voxels. This shift to working with the collective response may require less data for optimization purposes. The adjoint distribution will provide an importance distribution for source position and beam direction on the circular gantry surrounding the patient. However, because dose sensitivity information will no longer be for specific locations within a tissue type, additional data sets will need to be developed for example, a Green's function for the energy deposition. Future work will also explore how data from forward and adjoint simulations might be combined for a more efficient approach to treatment planning.

## III.F References:

[1] A. Brahme. "Optimization of Stationary and Moving Beam Radiation Therapy Techniques," *Radiotherapy and Oncology*, 12 (1988) 129-140.
[2] T.R. Mackie, T.W. Holmes, P.J. Reckwerdt, and J. Yang. "Tomotherapy: Optimized Planning and Delivery of Radiation Therapy," *International Journal of Imaging Systems and Technology*, Vol. 6, 43-55 (1995).
[3] Shepard, G. Olivera, L Angelos, O. Sauer, P. Reckwerdt, and T.R. Mackie, "A Simple Model for Examining Issues in Radiotherapy Optimization," *Medical Physics*, Vol. 26, 1212-1221 (1999).
[4] F. Difilippo, "Forward and Adjoint Methods for Radiotherapy Planning," *Medical Physics*, 25(9), 1702-1710, (1998).
[5] E.E. Lewis and W.F. Miller, *Computational Methods of Neutron Transport*, American Nuclear Society, Inc., La Grange Park, IL, 1993.

[6] Bell and Glasstone, *Nuclear Reactor Theory*, Krieger Publishing Co., Malabar, FL, 1970.
[7] F. Difilippo, M. Goldstein, B. Worley, and J. Ryman, "Adjoint Monte Carlo Methods for Radiotherapy Treatment Planning," Trans. Am. Nucl. Soc. 74, p.14-16 (June 1996).
[8] J. Lewins, *Importance: The Adjoint Function*, Pergamon Press, 1965
[9] Bell and Glasstone, *op. cit*.
[10] M.L. Williams, "Generalized Contributon Response Theory," *Nuclear Science and Engineering*, Vol. 108, 355-383, (1991).
[11] J.J. Duderstadt and L.J. Hamilton, *Nuclear Reactor Analysis*, Wiley, 1975.
[12] American National Standard ANSI/ANS-6.1.1-1977 *Neutron and Gamma-Ray Flux-to-Dose-Rate Factors* with permission of the publisher, the American Nuclear Society.
[13] M.L. Williams, "Generalized Contributon Response Theory," *Nuclear Science and Engineering*, Vol. 108, 355-383, (1991).
[14] D. Shepard, G. Olivera, L Angelos, O. Sauer, P. Reckwerdt, and T.R. Mackie, "A Simple Model for Examining Issues in Radiotherapy Optimization," *Medical Physics*, Vol. 26, 1212-1221 (1999).
[15] I. Rosen, R. Lane., S. Morril, and J. Belli, "Treatment Plan Optimization Using Linear Programming", *Medical Physics*, 18(2):141-152, 1990.
[16] GAMS Development Corporation, Washington DC, http://www.gams.com
[17] J.F. Briesmeister, Editor, *MCNP -- A General Monte Carlo N-Particle Transport Code version 4C*, Technical Report Number LA-13709-M, Los Alamos National Laboratory , Los Alamos, NM, (2000).
[18] J.C. Wagner, J.S. Hendricks, E.L. Redmond, S.P. Palmtag, A. Nagy, and P. Mendius, *MCNP: Multigroup/Adjoint Capabilities*, Technical Report No. LA-12704, Los Alamos National Laboratory, Los Alamos, NM, (1994).
[19] Energy spectrum courtesy of R. Jeraj, Ph.D., Tomotherapy Research Group, Department of Medical Physics, University of Wisconsin-Madison.

# III. Appendix:

### Conference Presentations and Publications

[1] S. Yoo[1], D. L. Henderson[2], and B. R. Thomadsen[1], "The Adjoint Method for the Optimization of Permanent Prostate Implant Patient Treatment Plans," in preparation for submission to the Journal of Medical Physics, November 2001.

[2] M. Kowalok[1], D. L. Henderson[2], and T. R Mackie[1], "An Investigation of the Adjoint Method for External Beam Radiation Therapy Treatment Planning using Monte Carlo Transport," Ninth International Conference on Nuclear Engineering (ICONE-9), April 8-12 2001, Nice Acropolis Center, Nice, France

[3] S. Yoo[1], D. L. Henderson[2], and B. R. Thomadsen[1], "Optimization of Prostate Cancer Treatment Plans using the Adjoint Transport Method and Discrete Ordinates Codes," Ninth International Conference on Nuclear Engineering (ICONE-9), April 8-12 2001, Nice Acropolis Center, Nice, France

[4] M. Kowalok[1], D. L. Henderson[2], and T. R Mackie[1], "Adjoint Monte Carlo Methods for Radiation Therapy Treatment Planning," Transactions of the American Nuclear Society, June 17-21, 2001, Milwaukee, Wisconsin

[5] S. Yoo[1], D. L. Henderson[2], and B. R. Thomadsen[1], "Optimization Treatment Planning for Interstitial Brachytherapy Using the Adjoint Transport Method," Transactions of the American Nuclear Society, June 17-21, 2001, Milwaukee, Wisconsin

[6] M. Kowalok[1], D. L. Henderson[2], and T. R Mackie[1], "An Adjoint Monte Carlo Method for External Beam Radiation Therapy Treatment Planning," 43rd Annual AAPM (American Association of Physicists in Medicine Meeting, July 22-26, 2001, Salt Lake City, Utah

[7] S. Yoo[1], D. L. Henderson[2], and B. R. Thomadsen[1], "Optimization in Permanent Prostate Implant Treatment Planning Using the Adjoint Dose Calculation and the Source Influence Fields," 43rd Annual AAPM (American Association of Physicists in Medicine) Meeting, July 22-26, 2001, Salt Lake City, Utah

[8] M. Kowalok[1], D. L. Henderson[2], and T. R Mackie[1], "An Investigation of the Adjoint Methods for External Beam Radiation Therapy Treatment Planning," AAPM North Central Chapter Spring Meeting, May 4, 2001, La Crosse, WI

[9] S. Yoo[1], D. L. Henderson[2], and B. R. Thomadsen[1], "Comparison of Forward and Adjoint Dose Calculations for the Optimization of Prostate Interstitial Brachytherapy Treatment Plans," AAPM North Central Chapter Spring Meeting, May 4, 2001, La Crosse, WI

---

[1]Department of Medical Physics, University of Wisconsin-Madison, 1530 Medical Sciences Center, Madison, WI
[2]Department of Engineering Physics, University of Wisconsin-Madison, 1500 Engineering Drive, Madison, WI